

A STATISTICAL SURVEY OF GEOMAGNETIC INDICES IN SOLAR CYCLE 23

ASIMOPOLOS Natalia-Silvia, ASIMOPOLOS Laurențiu,
BALEA Bogdan, ASIMOPOLOS Adrian-Aristide

Abstract. Based on the planetary geomagnetic indices in the Solar Cycle 23, which corresponds to the period 1996-2008, we performed a set of statistical tests, focused especially on major geomagnetic storms. For the analysis of the geomagnetic indices sampled from hour to hour, we started by eliminating the linear trend, in order to be as close as possible to the conditions of the stationary time series. According to the Box-Jenkins methodology, for the analysis of stationary time series, we used the autoregressive model (AR), mobile mediation (MA), autoregressive moving averages (ARMA) and integrated autoregressive moving averages (ARIMA), with the main goal to determine the model with the best fit of geomagnetic indices. The data for which we calculated this type of models are the hourly values of DST (disturbance storm time) and AE (Auroral electrojet), for the main geomagnetic storms in the Solar Cycle 23.

Keywords: DST (disturbance storm time), AE (Auroral electrojet), ARIMA (autoregressive integrated moving average, geomagnetic storm).

Rezumat. Studiul statistic al indicilor geomagnetici din Ciclul Solar 23. Pe baza indicilor geomagnetici planetari din ciclul solar 23, care corespunde perioadei 1996-2008, am efectuat un set de teste statistice, axate în special pe furtunile geomagnetice majore. Pentru analiza indicilor geomagnetici eșantionați de la oră la oră, am început prin eliminarea tendinței liniare, pentru a fi cât mai aproape de condițiile seriei de timp staționare. Conform metodologiei Box-Jenkins, pentru analiza seriilor de timp staționare, am folosit modelul autoregresiv (AR), mediere mobile (MA), medii mobile autoregresive (ARMA) și medii mobile autoregresive integrate (ARIMA), principalul obiectiv fiind determinarea modelului cu cea mai bună potrivire a indicilor geomagnetici. Datele pentru care am calculat acest tip de modele sunt valorile orare ale DST (timpul de furtună perturbator) și AE (electrojectul Auroral), pentru principalele furtuni geomagnetice din ciclul solar 23.

Cuvinte cheie: DST (timpul de furtună perturbator), AE (electroject auroral), ARIMA (medii mobile autoregresive integrate), furtună geomagnetică.

INTRODUCTION

Solar activity and the interaction of solar wind with the Earth's magnetosphere is a topic of utmost interest to the entire mankind, through the impact on life and activity on Earth. The scientific aspects related to these phenomena are approached both from an astrophysical, geophysical (BENOIT, 2012; ASIMOPOLOS et al., 2012; ASIMOPOLOS & ASIMOPOLOS, 2018) and mathematical (CHATFIELD, 1989; BISGAARD & KULAHCI, 2011; BOX et. al., 2016) point of view in many works and available data can be found on many websites (https://science.nasa.gov/science-news/science-at-nasa/2008/11jul_solarcycleupdate/, <http://sidc.oma.be/silso/> spotless, <http://www.intermagnet.org>, <http://www.noaa.gov>, <https://www.spaceweatherlive.com/en/archive/2015/08/28/kp>).

DATA USED

To obtain reliable AE indices it is desirable to use as many observatories as possible. However, there are two major difficulties: one is that the distribution of the observatories in operation is not uniform along the auroral zone, and the other is that the digitization of magnetograms is a laborious task.

The AE index is calculated from the geomagnetic variations in the horizontal component measured at selected observatories along the auroral zone in the northern hemisphere (<http://wdc.kugi.kyoto-u.ac.jp/dstae/format/aehformat.html>). To normalize the data, a baseline value for each station is first calculated for each month by averaging all the data from the station on the five international quietest days. The baseline value is subtracted from each value of one-minute data obtained at the station during that month. Then, among the data from all the stations at each given Universal Time, the largest and smallest values are selected. The AU and AL indices are respectively defined by the largest and the smallest values so selected. The difference, AU minus AL, defines the AE index, and the mean value of the AU and AL, i.e. $(AU + AL)/2$, defines the AO index. The term "AE indices" is usually used to represent these four indices (AU, AL, AE and AO). The AU and AL indices are intended to express the strongest current intensity of the eastward and westward auroral electrojets, respectively. The AE index represents the overall activity of the electrojets, and the AO index provides a measure of the equivalent zonal current.

For the calculation of the Dst index, four magnetic observatories, Hermanus, Kakioka, Honolulu, and San Juan are used. These observatories were chosen on the basis of the quality of observation and because their locations are sufficiently distant from the auroral and equatorial electrojets and they are distributed longitudinally as evenly as possible.

The baseline for H is defined for each observatory in a manner that takes into account the secular variation. For each observatory, the annual mean values of H, calculated from the five quietest day for each month, form the database for the baseline. The final Dst values are determined after each calendar year and therefore in this determination the annual mean values are available only up to and including the year for which the Dst is to be deduced. The baseline is expressed by a power series in time and the coefficients for terms up to the quadratic are determined by the method of least squares, using the annual means for the current year and the four preceding years.

SOLAR CYCLES AND GEOMAGNETIC STORMS DURING SOLAR CYCLE 23

The solar cycle denotes the solar magnetic activity cycle. This is a nearly periodic about 11-year change in the Sun's activity measured in terms of variations in the number of observed sunspots on the solar surface.

Table 1 includes data on Solar Cycles 1 to 24, beginning from 1600 to present.

Sunspots have been observed since the early 17th century and the sunspot time series represent the longest, continuously observed and recorded time series of any natural phenomena.

Solar activity, driven both by the sunspot cycle and transient aperiodic processes, governs the environment of the Solar System planets by creating space weather and impacts space- and ground-based technologies as well as the Earth's atmosphere and also possibly climate fluctuations on scales of centuries and longer.

Table 1. Solar Cycle (https://science.nasa.gov/science-news/science-at-nasa/2008/11jul_solarcycleupdate/, <http://sidc.oma.be/silso/spotless>).

Solar Cycle No.	Start (Minimum) (Year-Month)	Smoothed minimum ISN (start of cycle)	Maximum (Year-Month)	Smoothed maximum ISN	Time of Rise (years)	Duration (years)	Spotless days
1	1755-02	14.0	1761-06	144	6.3	11.3	
2	1766-06	18.6	1769-09	193	3.3	9.0	
3	1775-06	12.0	1778-05	264	2.9	9.3	
4	1784-09	15.9	1788-02	235	3.4	13.6	
5	1798-04	5.3	1805-02	82	6.8	12.3	
6	1810-08	0.0	1816-05	81	5.8	12.8	
7	1823-05	0.2	1829-11	119	6.5	10.5	
8	1833-11	12.2	1837-03	245	3.3	9.7	
9	1843-07	17.6	1848-02	220	4.6	12.4	
10	1855-12	6.0	1860-02	186	4.2	11.3	561
11	1867-03	9.9	1870-08	234	3.4	11.8	942
12	1878-12	3.7	1883-12	124	5.0	11.3	872
13	1890-03	8.3	1894-01	147	3.8	11.8	782
14	1902-01	4.5	1906-02	107	4.1	11.5	1007
15	1913-07	2.5	1917-08	176	4.1	10.1	640
16	1923-08	9.4	1928-04	130	4.7	10.1	514
17	1933-09	5.8	1937-04	199	3.6	10.4	384
18	1944-02	12.9	1947-05	219	3.3	10.2	382
19	1954-04	5.1	1958-03	285	3.9	10.5	337
20	1964-10	14.3	1968-11	157	4.1	11.4	285
21	1976-03	17.8	1979-12	233	3.8	10.5	283
22	1986-09	13.5	1989-11	214	3.2	9.9	257
23	1996-08	11.2	2001-11	180	5.3	12.3	619
24	2008-12	2.2	2014-04	116	5.3	<i>In progress</i>	1029 (30 Apr 2020)

A way to examine the length and depth of a solar minimum is by counting the number of days with no sunspots (spotless days). Spotless days never happen during the solar maximum but they do during the solar minimum.

The smoothed monthly number is average of monthly mean values over the 13 months (6 months before, 6 months after and baseline month). Extreme months are weighted with 1/2 and the rest are weighted by 1, according to the formula:

$$R_s = (0.5 R_{m-6} + R_{m-5} + R_{m-4} + R_{m-3} + R_{m-2} + R_{m-1} + R_m + R_{m+1} + R_{m+2} + R_{m+3} + R_{m+4} + R_{m+5} + 0.5 R_{m+6}) / 12$$

The longest minimum on record, was the Maunder Minimum of 1645-1715, which lasted 70 years. Sunspots were very rarely observed and that period of quietness coincided with the Little Ice Age, with a series of extraordinarily cold winters in Earth's northern hemisphere. In that period with low solar activity, volcanism was increased and also, possible changes in ocean current patterns ensued (Fig. 1).

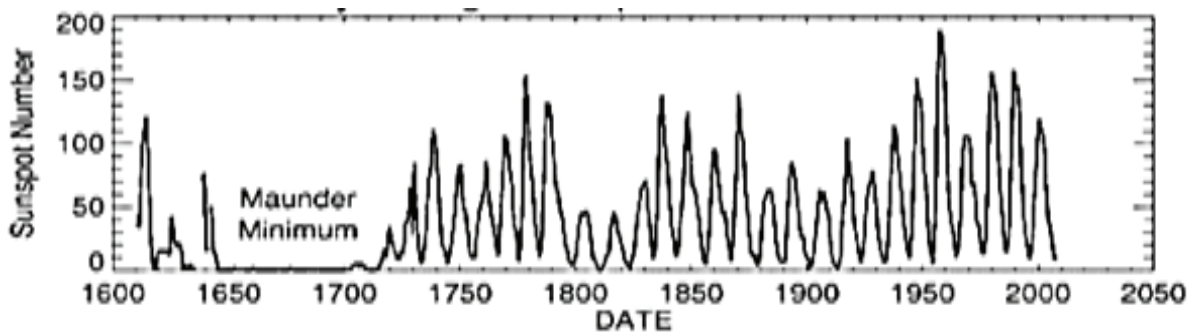


Figure 1. Yearly averaged Sunspot numbers between years 1610 and 2007 (https://science.nasa.gov/science-news/science-at-nasa/2008/11jul_solarcycleupdate/).

Fig. 2 shows the sunspot number during 1985-2020, where we can observe that the slope of increase from minimum to maximum is much steeper than the slope of decrease from maximum to minimum.

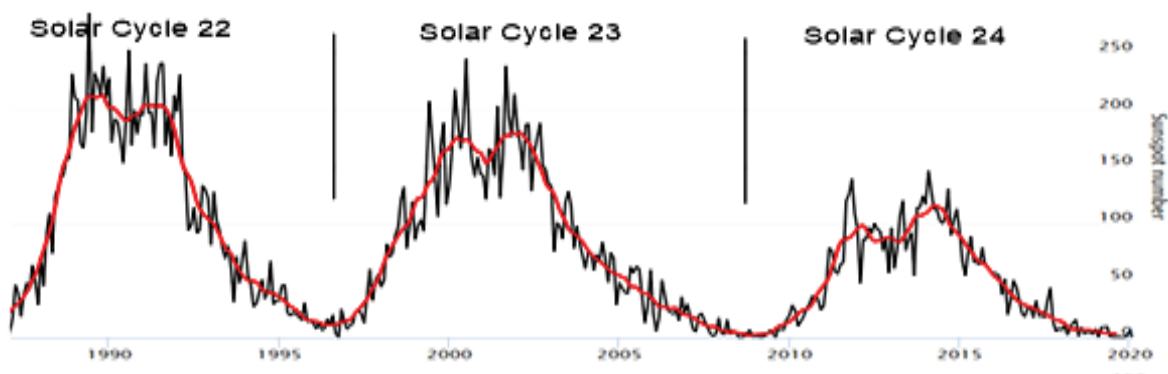


Figure 2. The last Solar Cycles 22-24 and Sunspot numbers (https://science.nasa.gov/science-news/science-at-nasa/2008/11jul_solarcycleupdate/).

Fig. 3 shows the number of sunspots during 2009-2020 years, where we can observe the monthly mean total sunspot number and the smoothed monthly total sunspots number.



Figure 3. The last Solar Cycle 24 in detail, sunspot numbers, monthly mean total sunspot number (black) and smoothed monthly total sunspots number (red) (https://science.nasa.gov/science-news/science-at-nasa/2008/11jul_solarcycleupdate/).

The start of the solar cycle 25 will be determined retrospectively. This determination cannot happen less than 7 months after the minimum to discount the possibility of a double trough. When the start of cycle 25 will be announced, a large number of spotless days that were sitting in cycle 24 will be transferred to cycle 25.

A geomagnetic storm occurs as a result of major disturbance of Earth's magnetosphere, when there is a very efficient exchange of energy from the solar wind into the space environment surrounding Earth. This is due to the variations in solar wind that produce major changes in the currents, plasmas, and fields in Earth's magnetosphere. The solar wind conditions that are effective for creating geomagnetic storms are sustained (for several to many hours) during periods of high-speed solar wind, and most importantly, a southward directed solar wind magnetic field (opposite the direction of Earth's field) at the dayside of the magnetosphere. This condition is effective for transferring energy from the solar wind into the Earth's magnetosphere.

The largest storms that result from these conditions are associated with solar coronal mass ejections (CMEs) where a billion tons or so of plasma from the sun, with its embedded magnetic field, arrives at Earth. CMEs typically take several days to arrive at Earth, but it has been observed that some of the most intense storms arrive in as short as 18 hours. Another solar wind disturbance that creates favourable conditions for geomagnetic storms is a high-speed solar wind stream that plots into the slower solar wind in front and creates co-rotating interaction regions. These regions are often related to geomagnetic storms that, while less intense than CME storms, can often deposit more energy in Earth's magnetosphere over a longer interval.

Table 2 presents the most 50 important geomagnetic storms from Solar Cycle 23, together with the three-hours geomagnetic indices Ap and Kp.

Table 2. Solar Cycle 23 - Top 50 geomagnetic storms
(<https://www.spaceweatherlive.com/en/auroral-activity/top-50-geomagnetic-storms/solar-cycle/23>).

No.	Date	Ap	00-03h	03-06h	06-09h	09-12h	12-15h	15-18h	18-21h	21-00h	Kp max
1	29/10/2003	204	5-	4	9	8	8-	8-	9-	9-	9
2	31/03/2001	192	7-	9-	9-	6+	7	8	8+	7+	9-
3	30/10/2003	191	9-	7+	5+	5-	5	7	9	9	9
4	27/07/2004	186	8+	8-	7+	8	9-	8+	6+	6	9-
5	15/07/2000	164	3	4-	5-	4+	8	9-	9	9-	9
6	10/11/2004	161	8-	8+	9-	8+	7+	6+	5+	4+	9-
7	25/07/2004	154	7	7+	6+	8-	7+	8	7+	7+	8
8	20/11/2003	150	1	4-	6+	6+	8-	9-	9-	8	9-
9	27/08/1998	144	8	8	8-	7-	7-	7-	7	6+	8
10	06/11/2001	142	9-	9-	7	5	5+	7-	6+	6+	9-
11	08/11/2004	140	9-	9-	8+	7	5	3-	4+	5+	9-
12	12/08/2000	123	5	7+	8-	8-	7+	7+	6+	4-	8-
13	09/11/2004	119	6-	6	5	6	7	7-	9-	7	9-
14	25/09/1998	117	8-	8	8+	7	6+	6-	3-	2+	8+
15	31/10/2003	116	8+	8-	7+	7-	7+	5-	4	4+	8+
16	05/10/2000	116	5+	7-	8-	7+	8-	7-	6+	5	8-
17	29/05/2003	109	4	4-	4-	3	7	8-	8+	8+	8+
18	18/08/2003	108	6-	6+	7	7-	7	7+	6+	6	7+
19	24/11/2001	104	3+	5+	8+	7	8-	7+	3	5-	8+
20	24/08/2005	102	3-	3+	6+	9-	7+	7-	6+	4+	9-
21	11/09/2005	101	6+	7	8-	6+	7	5+	6	5-	8-
22	04/05/1998	101	6	9-	8+	6-	6	4-	2+	3	9-
23	22/10/2001	96	7	5-	4-	6	6	7+	7	7	7+
24	15/12/2006	94	8+	8-	7-	6-	6	4	4	4-	8+
25	24/05/2000	93	8	8-	6	6-	5	5	6	4+	8
26	08/05/2005	91	6	5+	4-	6	8+	8-	5+	4-	8+
27	22/10/1999	91	7	8-	8	5+	5-	4+	6-	3+	8
28	30/05/2005	90	4	3+	6+	6+	7+	8-	7-	5-	8-
29	15/05/2005	87	6-	6-	8+	8-	4	4	5	5	8+
30	11/04/2001	85	3	2+	2	2	4-	8	8-	8+	8+
31	18/01/2005	84	7	6-	8-	6-	5+	5+	5	6-	8-
32	06/04/2000	82	2-	4+	3-	2+	3+	7-	8+	8+	8+
33	18/02/1999	80	5-	6	7-	7-	7-	5+	6	5	7-
34	23/05/2002	78	3-	3-	2	7-	8-	8+	5	3+	8+
35	12/09/2005	75	5-	4+	7	6-	5-	6	6	7	7
36	09/11/1998	75	5-	6-	7-	6+	6	5+	7-	5-	7-
37	20/03/2001	74	5-	6-	6	6-	7+	7	4+	4-	7+
38	07/04/2000	74	9-	6	6	4	4	4+	4-	4-	9-
39	17/09/2003	70	5+	5+	5	6+	7	5+	5	6-	7
40	20/04/2002	70	7	7+	6-	4+	5	6	5-	3-	7+
41	18/09/2000	70	8-	6-	5	6	6	6	3	3	8-
42	03/10/2001	69	5	3+	5	7	7-	7-	5-	5	7
43	01/10/2002	67	2-	3-	5-	6-	7-	7+	5-	7-	7+
44	21/01/2005	66	3+	2	2+	2+	3-	7-	8	7+	8
45	14/10/2003	66	3+	4	6-	5	4+	4+	7+	7+	7+
46	08/11/1998	66	6	8-	7+	5-	4	3+	3-	3+	8-
47	14/04/2006	65	4+	6	7-	7	5	5+	4	4+	7
48	22/01/2004	64	5	5	5	7	7-	4	5+	5-	7
49	04/10/2002	64	7+	6-	6	5-	4	4-	6+	4+	7+
50	08/06/2000	64	3-	4-	4+	6+	7	6+	6	5	7

Storms also result in intense currents in the magnetosphere, changes in the radiation belts, and changes in the ionosphere, including heating the ionosphere and upper atmosphere region called the thermosphere. In space, a ring of westward current around Earth produces magnetic disturbances on the ground. A measure of this current, the

disturbance storm time (Dst) index, has been used historically to characterize the size of a geomagnetic storm. In addition, there are currents produced in the magnetosphere that follow the magnetic field, called field-aligned currents, and these connect to intense currents in the auroral ionosphere. These auroral currents, called auroral electrojets, also produce large magnetic disturbances. Together, all of these currents, and the magnetic deviations they produce on the ground, are used to generate a planetary geomagnetic disturbance index called Kp. This index is the basis for one of the three NOAA Space Weather Scales, the Geomagnetic Storm, or G-Scale, that is used to describe space weather that can disrupt systems on Earth.

During storms, the currents in the ionosphere, as well as the energetic particles that precipitate into the ionosphere add energy in the form of heat that can increase the density and distribution of density in the upper atmosphere, causing extra drag on satellites in low-earth orbit. The local heating also creates strong horizontal variations in the ionospheric density that can modify the path of radio signals and create errors in the positioning information provided by GPS. While the storms create beautiful aurora, they can also disrupt navigation systems such as the Global Navigation Satellite System (GNSS) and create harmful geomagnetic induced currents (GICs) in the power grid and pipelines.

AUTO-REGRESSIVE INTEGRATED MOVING AVERAGE (ARIMA)

Related with the Box-Jenkins theory, ARIMA(p, d, q) forecasting equation: ARIMA models are, in theory, the most general class of models for forecasting a time series which can be made to be “stationary” by linearization, differentiation (if necessary) or perhaps in conjunction with nonlinear transformations. A random variable that is a time series is stationary if its statistical properties are all constant over time. A stationary series has no trend, its variations around its mean have a constant amplitude, and it wiggles in a consistent fashion, i.e., its short-term random time patterns always look the same in a statistical sense. The latter condition means that its autocorrelations (correlations with its own prior deviations from the mean) remain constant over time, or equivalently, that its power spectrum remains constant over time. A random variable of this form can be viewed usually as a combination of signal and noise, and the signal could be a pattern of fast or slow mean reversion, or sinusoidal oscillation, or rapid alternation in sign, and it could also have a seasonal component. An ARIMA model can be viewed as a “filter” that tries to separate the signal from the noise, and the signal is then extrapolated into the future to obtain forecasts.

The ARIMA forecasting equation for a stationary time series is a linear equation of regression-type in which the predictors consist of lags of the dependent variable and/or lags of the forecast errors. That is:

The predicted value of Y = a constant and/or a weighted sum of one or more recent values of Y and/or a weighted sum of one or more recent values of the errors.

If the predictors consist only of lagged values of Y, it is a pure autoregressive (“self-regressed”) model, which is just a special case of a regression model and which could be fitted with standard regression software.

The lags of the stationarized series in the forecasting equation are referred to as “autoregressive” terms, lags of the forecast errors are called “moving average” terms, and a time series which needs to be differenced to be made stationary is said to be an “integrated” version of a stationary series. Random-walk and random-trend models, autoregressive models, and exponential smoothing models are all special cases of ARIMA models.

A non-periodical ARIMA model is classified as an “ARIMA(p, d, q)” model, where:

- p is the number of autoregressive terms,
- d is the number of non-periodical differences needed for stationarity, and
- q is the number of lagged forecast errors in the prediction equation.

The forecasting equation is constructed as follows. First, let y_t denote the d^{th} difference of Y, which means:

$$\text{If } d=0: y_t = Y_t$$

$$\text{If } d=1: y_t = Y_t - Y_{t-1}$$

$$\text{If } d=2: y_t = (Y_t - Y_{t-1}) - (Y_{t-1} - Y_{t-2}) = Y_t - 2Y_{t-1} + Y_{t-2}$$

The second difference of Y (the $d=2$ case) is not the difference from 2 periods ago. Rather, it is the *first-difference-of-the-first difference*, which is the discrete analogue of a second derivative, i.e., the local acceleration of the series rather than its local trend.

In terms of y_t , the general forecasting equation is:

$$\hat{y}_t = \mu + \phi_1 y_{t-1} + \dots + \phi_p y_{t-p} - \theta_1 e_{t-1} - \dots - \theta_q e_{t-q}$$

Here, the moving average parameters (θ 's) are defined so that their signs are negative in the equation, following the convention introduced by Box and Jenkins. While the underlying concepts are fairly straightforward, a number of challenges arise in practice. In particular, the distribution theory for parameter estimates and associated test statistics developed for stationary time series do not apply when a unit root is present in the model. The asymptotic distributions are functions of standard Brownian motions and do not have convenient closed-form expressions. As a result, the percentiles of the distributions needed to perform the tests have to be evaluated using numerical approximations or by simulation. Moreover, the form of the test statistics and their asymptotic distributions are

impacted by the presence of deterministic terms such as constants or time trends in the model. The size and power characteristics of unit root tests can also be a concern for shorter time series.

A Code in Matlab for calculating an ARIMA model is presented in the annex (<https://www.mathworks.com>).

The largest geomagnetic storm (Fig. 4) in SC23 began with a series of powerful solar flares and associated geoeffective Coronal Mass Ejections (CMEs) traveling at 2000km / s drove shock fronts that impacted the Earth's magnetic field consecutively on October 29 and 30, resulting in intense geomagnetic disturbances during 29–31 October.

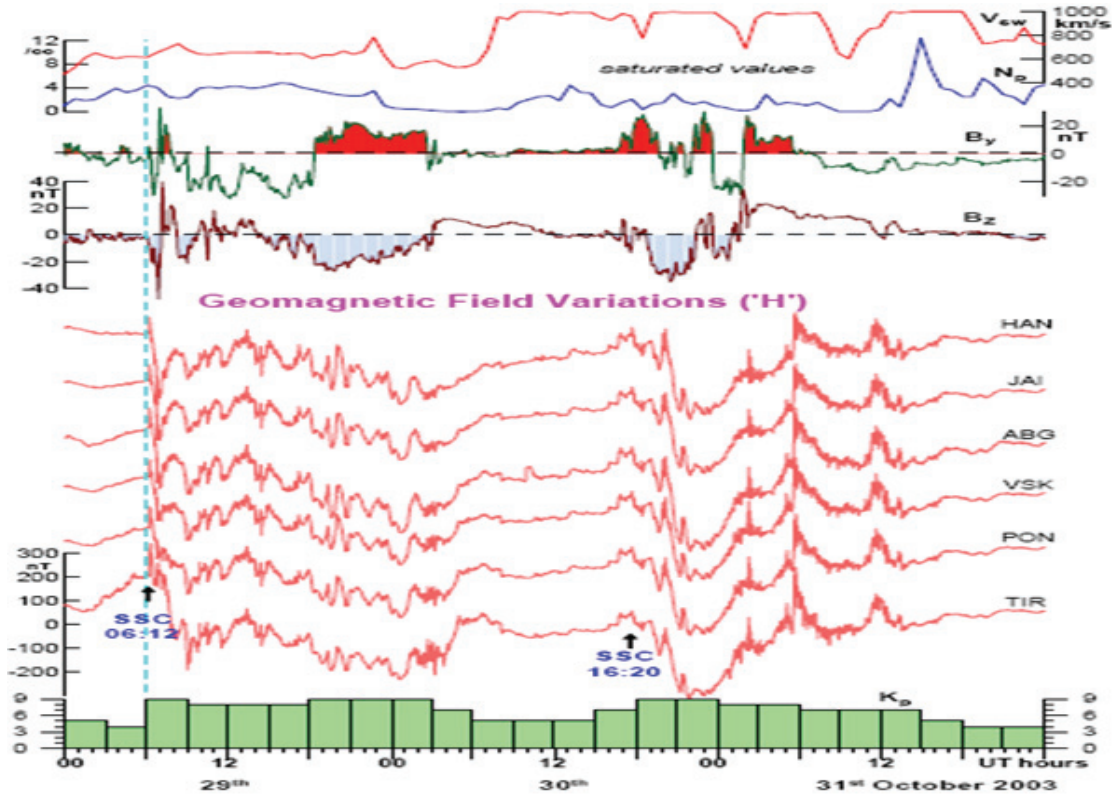


Figure 4. Geomagnetic and astrophysical parameters during 29-31 October 2003.

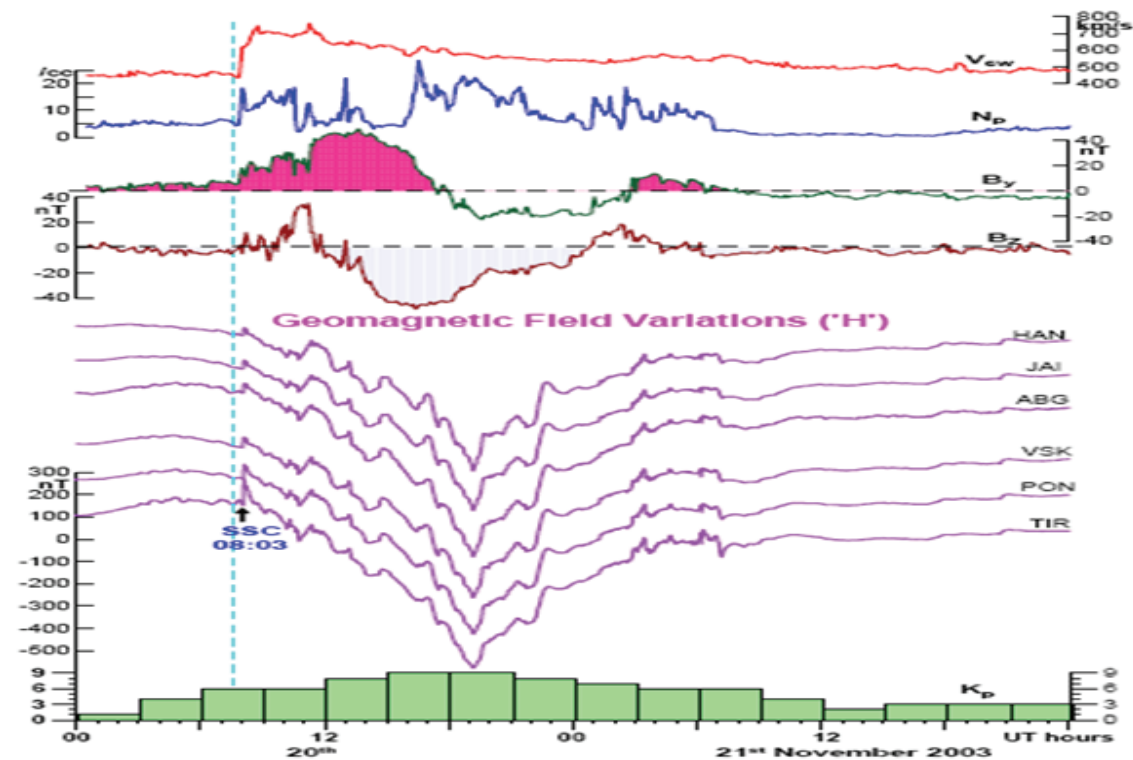


Figure 5. Geomagnetic and astrophysical parameters during 20-21 November 2003

Another intense geomagnetic storm activity (Fig. 5) occurred during 20–21 November, resulting from a solar flare that had an associated geoeffective CME travelling at a speed of 1100 km/s.

Digital ground magnetic field measurements from the equatorial and low-latitude locations in conjunction with the interplanetary solar wind and magnetic field parameters are used to study the characteristics of these storms.

CONCLUSIONS

The Dst index represents the axially symmetric disturbance magnetic field at the dipole equator on the Earth's surface. Major disturbances in Dst are negative, namely decreases in the geomagnetic field. These field decreases are produced mainly by the equatorial current system in the magnetosphere, usually referred to as the ring current. The neutral sheet current flowing across the magnetospheric tail makes a small contribution to the field decreases near the Earth. Positive variations in Dst are mostly caused by the compression of the magnetosphere from solar wind pressure increases.

There is some correlation between DST and the AE indices. The derivation procedure essentially consists of the following four steps:

- Subtraction of the geomagnetic main field and the Sq (solar quiet daily variation) field to calculate the disturbance field component.

- Coordinate transformation to a dipole coordinate system.

- Calculation of the longitudinally symmetric component (i.e. six station average) and the asymmetric component (i.e. disturbance field minus the symmetric component).

- Derivation of the asymmetric indices (i.e. the range between the maximum and the minimum asymmetric fields).

However, any selection of quiet days would introduce arbitrariness. Also, Sq is a dynamic variation which often changes over time periods of a few hours to several days, and therefore, the modelling of Sq has a statistical meaning only. Thus, the internationally selected five quietest days of each month were used. A statistical study can readily be made on these quiet days and if necessary, corrections can be applied to the Dst index for any modifications on Sq.

An ARIMA model can be viewed as a “filter” that tries to separate the signal from the noise, and the signal is then extrapolated into the future to obtain forecasts.

Forecasting time series data is an important subject in many domains, inclusive in geomagnetism. Traditionally, there are several techniques to effectively forecast the next lag of time series data such as univariate Auto Regressive (AR), univariate Moving Average (MA), Simple Exponential Smoothing (SES), and more notably Auto Regressive Integrated Moving Average (ARIMA) with its many variations. In particular, the ARIMA model has demonstrated its outperformance in precision and accuracy of predicting the next lags of time series.

Understanding the activity of Sun and predicting the sunspot cycle and strong geomagnetic storms are grand challenges in astrophysics in order to understand magnetohydrodynamic phenomena elsewhere in the Universe.

This cyclicity of Sun has major ramifications for space science and human activities on Earth.

ACKNOWLEDGEMENT

We gratefully acknowledge the many and significant contributions and comments provided by our colleagues from geomagnetic observatories. The manual about observatories methodologies is based on the original document (INTERMAGNET Technical Reference).

Also, we thank the Ministry of Research for the financial support provided to the project: “The realization of 3D geological / geophysical models for the characterization of some areas of economic and scientific interest in Romania”, Contract no. 28N / 2019 and project Nr.16PCCDI/2018: “Institutional capacities and services for research, monitoring and forecasting of risks in extra-atmospheric space”, within PNCDIII.

REFERENCES

- ASIMOPOLOS N. S. & ASIMOPOLOS L. 2018. Study on the high-intensity geomagnetic storm from march 2015, based on terrestrial and satellite data. *Micro and Nano Tehnologies & Space Tehnologies & Planetary Science*. Issue 6.1, SGEM 2018. București. **18**: 593-600. ISBN 978-619-7408-50-8, ISSN 1314-2704, DOI: 10.5593/sgem2018/6.1.
- ASIMOPOLOS L., SĂNDULESCU A. M., ASIMOPOLOS N. S., NICULICI E. 2012. *Analysis of data from Surlari National Geomagnetic Observatory*. Edit. Ars Docendi. București. 96 pp.
- BOX G. E. P., JENKINS G. M., REINSEL G. C., LJUNG G. M. 2016. *Time series analysis - Forecasting and Control*. Fifth Edition. John Wiley & Sons. Hoboken. New Jersey. 709 pp.
- BISGAARD S. & KULAHCI M. 2011. *Time series analysis and forecasting by example*. John Wiley & Sons. Hoboken. New Jersey. 382 pp.
- BENOIT S. L. 2012. *INTERMAGNET Technical reference manual - Version 4.6*. Murchison House West Mains Road Edinburgh EH9 3LA UK. 100 pp.
- CHATFIELD C. 1989. *The Analysis of Time Series: An Introduction*. Chapman & Hall. 241 pp.

- ***. https://science.nasa.gov/science-news/science-at-nasa/2008/11jul_solarcycleupdate/, (accessed February, 2020).
 ***. <http://sidc.oma.be/silso/spotless> (accessed February, 2020).
 ***. <https://www.spaceweatherlive.com/en/auroral-activity/top-50-geomagnetic-storms/solar-cycle/23> (accessed February, 2020).
 ***. <http://www.intermagnet.org> (accessed February, 2020).
 ***. <http://www.noaa.gov> (accessed February, 2020).
 ***. <https://www.spaceweatherlive.com/en/archive/2015/08/28/kp> (accessed February, 2020).
 ***. <https://www.mathworks.com> (accessed February, 2020).

ANNEX

Matlab code for ARIMA:

```
STSFMs_ARIMA.AR = [];
STSFMs_ARIMA.MA = [];
Lags = num2cell(nan(1,STSFMs_ARIMA.Seasonality));
STSFMs_ARIMA.SAR = Lags;
STSFMs_ARIMA.SMA = Lags;
else
    STSFMs_ARIMA = arima('SMALags',12,'D',1,'SARLags',12,...
        'Seasonality',12);
    D1 = LagOp({1 -1},'Lags',[0,1]);
    D12 = LagOp({1 -1},'Lags',[0,12]);
    D = D1*D12;
    dFinal_test = filter(D,Final_test);
    STSFMs_ARIMA_1 = arima('SMALags', 12, 'D',1,'SARLags',12,'MALags',1,'ARLags',1,...
        'Seasonality',12);
    STSFMs_ARIMA_Minitab = arima('SMALags', 12,'SMA',0.9852,
    D',1,'SARLags',12,'SAR',0.1264,'MALags',1,'MA',0.0500,'ARLags',1,'AR',0.9688,...
        'Seasonality',12,'Constant',-0.0002256,'Variance',2);
    max_order = 3;
    [aic_matrix,bic_matrix] = ARMA_model_order_tuning(Final_test,max_order);
end
```

Asimopolos Natalia-Silvia

Geological Institute of Romania
 1st Caransebeș Street, 012271 - Bucharest, Romania.
 E-mail: natalia.asimopolos@igr.ro, asi_nata@yahoo.com

Asimopolos Laurențiu

Geological Institute of Romania
 1st Caransebeș Street, 012271 - Bucharest, Romania.
 E-mail: laurentiu.asimopolos@igr.ro, asimopolos@gmail.com

Balea Bogdan-Valeriu

Geological Institute of Romania
 1st Caransebeș Street, 012271 - Bucharest, Romania.
 E-mail: natalia.asimopolos@igr.ro, asi_nata@yahoo.com

Asimopolos Adrian Aristide

University POLITEHNICA of Bucharest
 Faculty of Transports, 313 Splaiul Independentei, 060042 - Bucharest, Romania.
 E-mail: adrian.asimopolos@gmail.com

Received: March 28, 2020
 Accepted: August 12, 2020